Modern radio engineering and telecommunication systems
Современные радиотехнические и телекоммуникационные системы

UDC 621.314.1+681.586.7
https://doi.org/10.32362/2500-316X-2025-13-2-36-45
EDN TIPRXB

RESEARCH ARTICLE

Zeta topology DC/DC converter design based on TPS40200 driver

Vladimir K. Bityukov [1],
Aleksey I. Lavrenov [1, @],
Daniil A. Malitskiy [2]

[1] *MIREA – Russian Technological University, Moscow, 119454 Russia*
[2] *Sputniks, Moscow, 121205 Russia*
[@] *Corresponding author, e-mail: lavrenov@mirea.ru*

Abstract
Objectives. The study set out to investigate typical characteristics of a Zeta converter developed by the authors based on the TPS40200 driver under various input voltages and loads and compare the experimental characteristics of the Zeta converter with those obtained through SPICE[1] simulation in the *Multisim* computer-aided design (CAD) system, as well as with the results derived from a continuous-time mathematical model.
Methods. A continuous-time mathematical model of the Zeta converter and the *Multisim* CAD system were used. The schematic diagram of the converter was developed according to the TPS40200 driver circuit design methodology presented in its datasheet. The printed circuit board layout was created using the *Altium Designer* CAD system.
Results. An experimental test bench of the Zeta topology DC/DC converter was designed and built using coupled chokes based on the TPS40200 driver. The results of the study showed a high correlation of both its load characteristics and its DC and AC components of currents flowing through the choke windings and capacitor voltages from the input voltage at two load resistances of 50 and 100 Ohm obtained by experimental, computational, and modeling methods.
Conclusions. The continuous-time mathematical model of the converter, along with the calculation method based on it, forms a foundation for the design of DC/DC converters using the Zeta topology. The experiment confirms the validity of both the mathematical model and the calculation method. The proposed design methods takes the magnetic coupling and the active resistance of inductors into account. The magnetic coupling permits a two-fold reduction of inductor values while maintaining the same ripple or a reduction in the ripple by up to half with unchanged inductor values.

Keywords: DC/DC converter, Zeta topology, converter, mathematical model, design method, TPS40200, Altium Designer, Multisim, printed circuit board

[1] SPICE (Simulation Program with Integrated Circuit Emphasis) is an open source simulator of general-purpose electronic circuits.

• **Submitted:** 05.06.2024 • **Revised:** 16.08.2024 • **Accepted:** 06.02.2025

For citation: Bityukov V.K., Lavrenov A.I., Malitskiy D.A. Zeta topology DC/DC converter design based on TPS40200 driver. *Russian Technological Journal.* 2025;13(2):36–45. https://doi.org/10.32362/2500-316X-2025-13-2-36-45, https://elibrary.ru/TIPRXB

Financial disclosure: The authors have no financial or proprietary interest in any material or method mentioned.

The authors declare no conflicts of interest.

НАУЧНАЯ СТАТЬЯ

Проектирование DC/DC-преобразователя, построенного по Zeta-топологии на базе драйвера TPS40200

В.К. Битюков [1],
А.И. Лавренов [1, @],
Д.А. Малицкий [2]

[1] *МИРЭА – Российский технологический университет, Москва, 119454 Россия*
[2] *ООО «СПУТНИКС», Москва, 121205 Россия*
[@] *Автор для переписки, e-mail: lavrenov@mirea.ru*

Резюме

Цели. Целью работы является исследование типовых характеристик разработанного Zeta-преобразователя на основе драйвера TPS40200 (Texas Instruments, США) при различных входных напряжениях и нагрузках и сравнение экспериментальных характеристик Zeta-преобразователя с аналогичными, полученными при помощи SPICE[1]-моделирования в системе автоматизированного проектирования (САПР) *Multisim*, а также с помощью предельной непрерывной математической модели.

Методы. Использована предельная непрерывная математическая модель Zeta-преобразователя и САПР *Multisim*. Принципиальная электрическая схема преобразователя разработана по методике расчета обвязки драйвера TPS40200, представленной в его технической документации. С использованием САПР *Altium Designer* произведена разводка печатной платы.

Результаты. Спроектирован и создан экспериментальный стенд DC/DC-преобразователя, построенного по Zeta-топологии со связанными дросселями на базе драйвера TPS40200. Результаты исследования показали высокую корреляцию как его нагрузочных характеристик, так и его постоянных и переменных составляющих токов, протекающих через обмотки дросселей, и напряжений на конденсаторах от входного напряжения при двух сопротивлениях нагрузки 50 и 100 Ом, полученных различными методами: экспериментальным, расчетным и моделированием.

Выводы. Предельная непрерывная математическая модель преобразователя и метод расчета, основанный на ней, являются базой для проектирования DC/DC-преобразователей, построенных по топологии Zeta. Экспериментально доказана достоверность математической модели, а также метода проектирования. Предложенный метод проектирования позволяет учесть магнитную связь и активное сопротивление обмоток дросселей. Учет магнитной связи позволяет уменьшить номиналы дросселей до двух раз при неизменных пульсациях либо уменьшить пульсации до двух раз при неизменных номиналах дросселей.

Ключевые слова: DC/DC-преобразователь, топология Zeta, преобразователь, математическая модель, метод проектирования, TPS40200, Altium Designer, Multisim, печатная плата

[1] SPICE (англ. Simulation Program with Integrated Circuit Emphasis) – программа-симулятор электронных схем общего назначения с открытым исходным кодом. [SPICE (Simulation Program with Integrated Circuit Emphasis) is an open source simulator of general-purpose electronic circuits.]

• **Поступила:** 05.06.2024 • **Доработана:** 16.08.2024 • **Принята к опубликованию:** 06.02.2025

Для цитирования: Битюков В.К., Лавренов А.И., Малицкий Д.А. Проектирование DC/DC-преобразователя, построенного по Zeta-топологии на базе драйвера TPS40200. *Russian Technological Journal*. 2025;13(2):36–45. https://doi.org/10.32362/2500-316X-2025-13-2-36-45, https://elibrary.ru/TIPRXB

Прозрачность финансовой деятельности: Авторы не имеют финансовой заинтересованности в представленных материалах или методах.

Авторы заявляют об отсутствии конфликта интересов.

INTRODUCTION

A relevant trend in the development of modern autonomous radio devices involves a reduction in mass-dimensional parameters and accompanying improvement in the tactical and technical characteristics of the power converters used in them [1–3]. Traditionally, choke DC/DC converters of various topologies are used to power such devices [4–6]. In topologies where two chokes are used for energy storage and transmission, it has long been common practice to use coupled chokes to reduce their mass-dimensional parameters and improve basic stabilizer characteristics [7, 8]. Examples of modern devices based on coupled chokes are given in [9, 10]. The design of such converters is typically based on their mathematical models [11–15]. The converter based on the calculation method proposed in [16] was validated by comparing the calculated characteristics with the modeling results rather than via an empirical study. To remedy this deficiency, we set out to experimentally study the DC/DC converter based on the Zeta topology with coupled chokes.

1. SCHEMATIC DIAGRAM OF THE CONVERTER BASED ON THE TPS40200 DRIVER

A TPS40200 microcircuit (Texas Instruments, USA) was chosen as the driver for the Zeta converter for a number of reasons. Firstly, this driver can deliver up to 95% efficiency at various load currents and over a wide range of input and output voltages[1]. Secondly, the chip has a fairly simple design with all the necessary functionality configured via external circuitry. Although this functionality is not declared by the manufacturer, this allows the driver to be used to control Zeta converters. Thirdly, an important factor in choosing this particular driver is its price and availability.

The circuit diagram of the DC/DC converter based on the TPS40200 driver is made up of two functional parts that are calculated separately (Fig. 1). The first part, responsible for the device logic, is the TPS40200 driver and all adjacent elements. The second is the power part of the converter based on Zeta topology, responsible for DC conversion. The nominal values of the elements of the Zeta topology are calculated using the design method [16], which is based on the continuous-time mathematical model of the converter.

A sawtooth signal of the required frequency is formed on the first pin of the RC driver TPS40200 using the frequency setting circuit R1C1. The switching frequency of the VT1 power switch is selected to be 500 kHz. However, the actual switching frequency may vary due to variations in basic parameters of electronic components within technological tolerances.

The part of the circuit responsible for the Zeta converter input current threshold consists of the current sensing resistor R7 and the smoothing filter R6C6, which is necessary to reduce the influence of the high-frequency component occurring when the power switch VT1 is switched. C2 is a start-up capacitor that determines the start-up time of 9 ms. C3C4R2 is a frequency compensation chain whose cut-off frequency is approximately 6–10 times lower than the switching frequency.

In the circuit diagram, the PLS-40 pins labelled “TP” and “P” are intended for the monitoring of currents and voltages, respectively.

2. ARRANGING THE ZETA CONVERTER PCB LAYOUT

The printed circuit board (PCB) layout is arranged in the *Altium Designer* computer-aided design (CAD) system[2], taking into account requirements for easy soldering and convenient multimeter or oscilloscope measurement (Figs. 2 and 3).

[1] TPS40200 Datasheet. TPS40200 Wide Input Range Non-Synchronous Voltage Mode Controller datasheet (Rev. G). Texas Instruments. SLUS659G–FEBRUARY 2006–REVISED NOVEMBER 2014.

[2] https://www.altium.com/altium-designer. Accessed May 24, 2024.

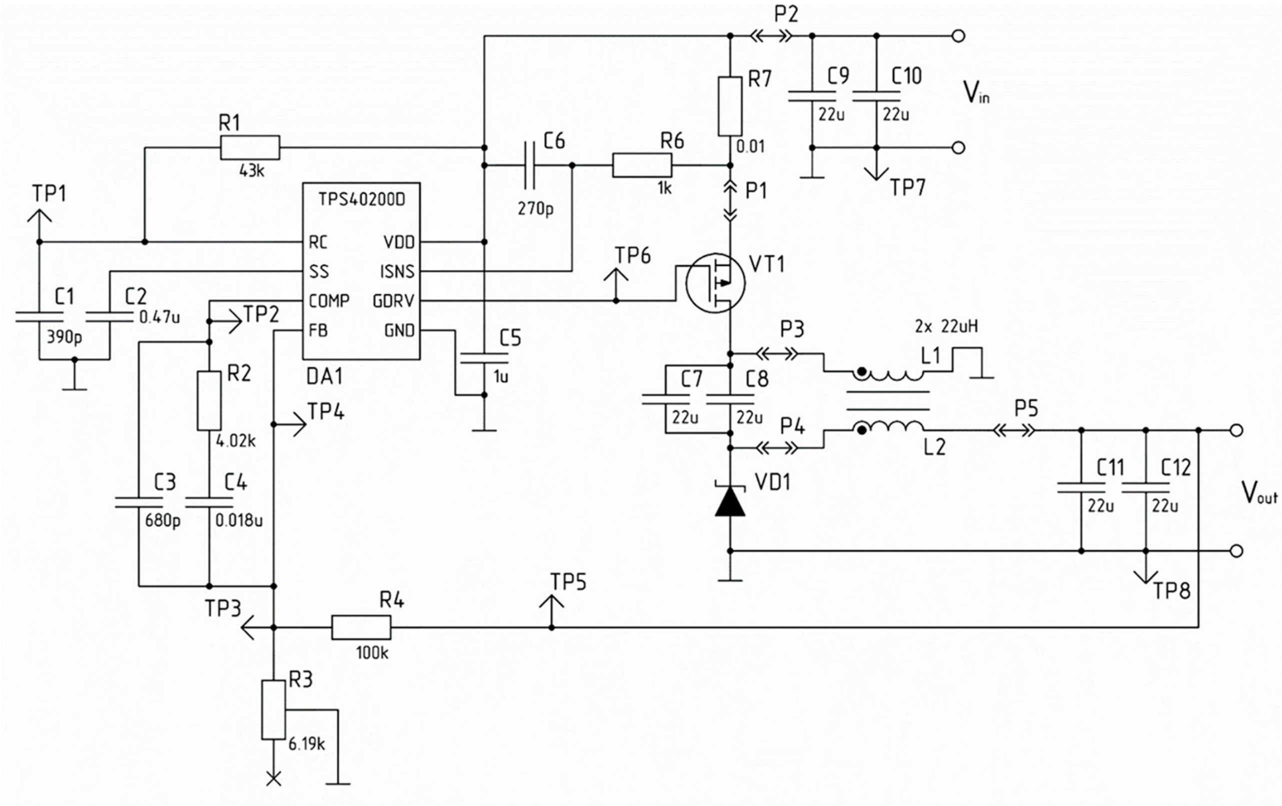

Fig. 1. Circuit diagram of a step-up and step-down DC/DC converter based on the Zeta topology. Here and in the following figures, the designations of the circuit elements correspond to those adopted in GOST 2.710-81[3]

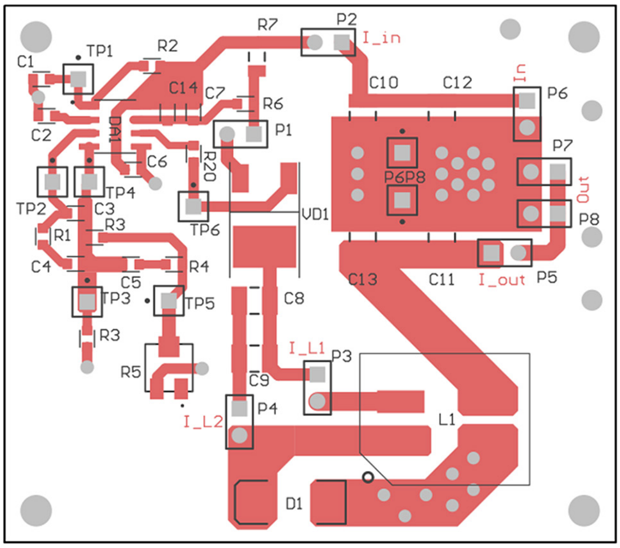

Fig. 2. Upper PCB layer

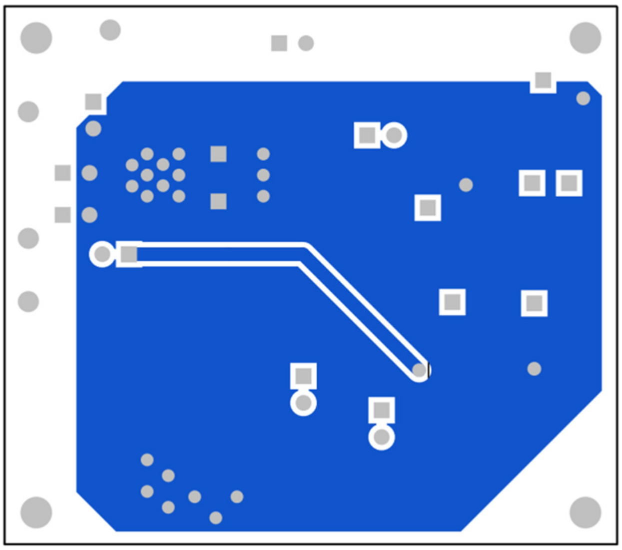

Fig. 3. Lower PCB layer

The VT1 transistor is a WMO25P06T1 p-channel MOSFET (Wayon Electronics Co., China) with a maximum power dissipation of up to 2.5 W and dynamic characteristics that allow operation with a switching frequency of up to 1 MHz.[4] The TPS40200 chip, having a high input voltage of up to 52 V, variable switching frequency of up to 500 kHz, and a gate current of up to 300 mA, is used as the transistor driver. This allows the gate voltage rise time (edge duration) of the transistor to be 0.025–0.040 µs.

[3] GOST 2.710-81. Interstate Standard. *Unified system for design documentation. Alpha-numerical designations in electrical diagrams*. Moscow: Standartinform; 2008 (in Russ.).

[4] WMO25P06T1 Datasheet. 60V P-Channel Enhancement Mode Power MOSFET. Rev. 3.0, 2020. P. 6.

The footprint inductance over the average width (2 mm) of the path from the transistor drain to the positive output pole is 0.3 nH/mm, while the path length is ~60 mm, corresponding to an inductance of 20 nH.

The interlayer capacitance is approximately 60 pF/cm^2. Taking into account the discrete element ratings, the influence of parasitic components on the device parameters is minimal. The considerable thickness of the dielectric has a major influence due to the weakness of the coupling of the signal lines in the upper layer to the lower ground layer, which can lead to significant cross-interference, especially in the feedback circuit.

The operating frequency of the converter is approximately 500 kHz, which is equivalent to a wavelength of 600 m. This is much larger than the PCB size and the length of the conductors.

A general view of the developed PCB with components is shown in Fig. 4.

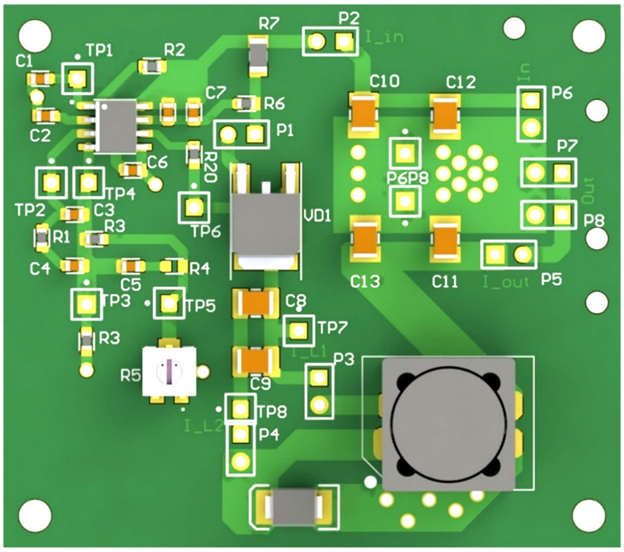

Fig. 4. General view of the developed PCB with components

The substrate material used in the PCB (Rezonit, Russia) is FR4 Tg135 with a relative dielectric constant of 4.3 and a thickness of 1.93 mm. The metallization thickness is 0.035 mm. PCB type: double-sided. PCB dimensions: 58 × 51 mm.

3. EXPERIMENTAL STUDY OF ZETA CONVERTER BASED ON TPS40200 DRIVER

The study was carried out at the Department of Radio Wave Processes and Technologies of the Institute of Radioelectronics and Informatics at RTU MIREA. The test bench shown in Fig. 5 consists of a Zeta converter, a PC, a laboratory power supply, an oscilloscope, a multimeter, a current sensor, and a set of samples/wires for connecting the PCB. The instruments and hardware used for the study, namely, the NGE100 power supply, the RTB2002 oscilloscope, and the HMC8012 universal multimeter, are from Rohde & Schwarz (Germany).[5]

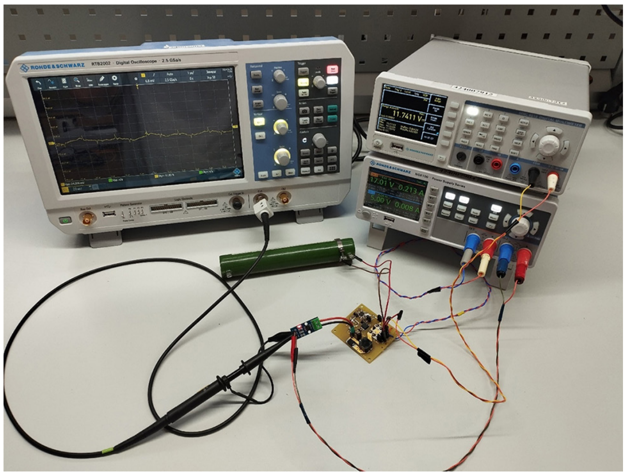

Fig. 5. Test bench for experimental study

The test bench is designed for experimental study of the typical characteristics of a DC/DC converter, with which similar characteristics can be compared as obtained by the design method based on the continuous-time mathematical model of the converter and by the simulation method using *Multisim* CAD.[6]

Typical characteristics of converters traditionally include the load characteristic (LC), which is the dependence of its output voltage U_{out} on the load current I_L at constant input voltage U_{in}, i.e., $U_{out} = f(I_L)$ with U_{in} = const, as well as the dependence of the constant and variable components of currents i_{L1}, i_{L2} and voltages $u_{C7, C8}$, $u_{C11, C12}$ on the input voltage U_{in} at different load resistances.

The converter LCs obtained in the experimental study at input voltages of 6.5, 12.0, and 17.5V are shown in Figs. 6–8.

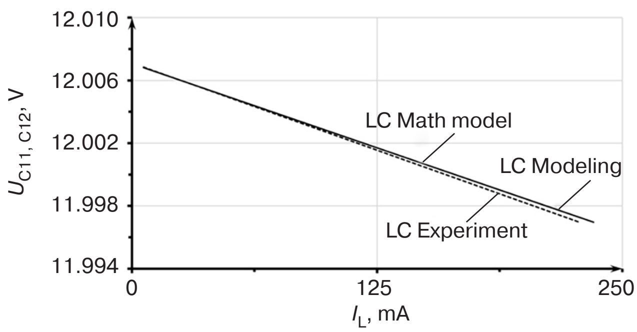

Fig. 6. Load characteristic at an input voltage of 6.5 V

5 https://www.rohde-schwarz.com/. Accessed July 11, 2024.

6 https://www.ni.com/ru-ru/shop/product/multisim.html. Accessed February 19, 2024.

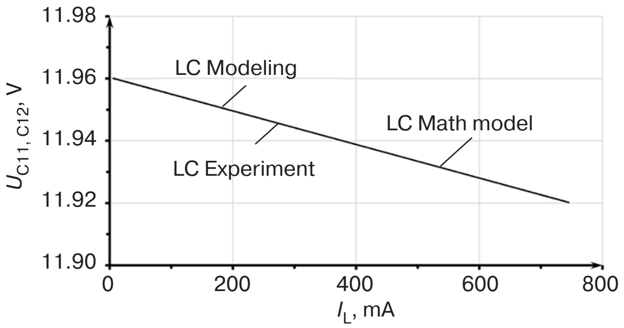

Fig. 7. Load characteristic at an input voltage of 12.0 V

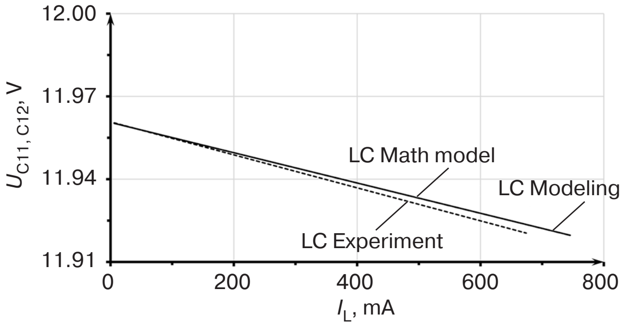

Fig. 8. Load characteristic at an input voltage of 17.5 V

Since the constant charging current of the output capacitor is negligible compared to the load current, the current of the second choke can be assumed to be equal to the load current $I_{L2} = I_L$. The deviation of the experimental load current I_L (Figs. 6–8) from the calculated value does not exceed 10% for an input voltage of 17.5 V. It should be noted that the maximum deviation is 3% for an input voltage of 6.5 V and 4% for 12.0 V.

The results of the study of the dependence of the constant and variable components of the currents i_{L1}, i_{L2} and the voltages $u_{C7, C8}$, $u_{C11, C12}$ on the input voltage U_{in} for two load resistances of 50 and 100 Ohm are shown in Figs. 9–16.

A good agreement between the experimental and calculated values is shown by the graphs of the dependence of the constant currents flowing through the windings of the chokes L1 and L2 on the input voltage U_{in} (Fig. 9) and of the voltages across the capacitors C7, C8 and C11, C12 on the input voltage U_{in} (Fig. 10) at a load resistance of 50 Ohm. The deviation in the constant components for the I_{L1} current amounts to 13% on average, while the deviation in the I_{L2} current is 15%, and the deviation in the $U_{C11, C12}$ voltage comprises 0.27%. The difference values obtained for the ripple spreads of corresponding currents and voltages obtained in the same way are as follows: Δi_{L1} is 5%, Δi_{L2} is 21%, while $\Delta u_{C11, C12}$ is 15%.

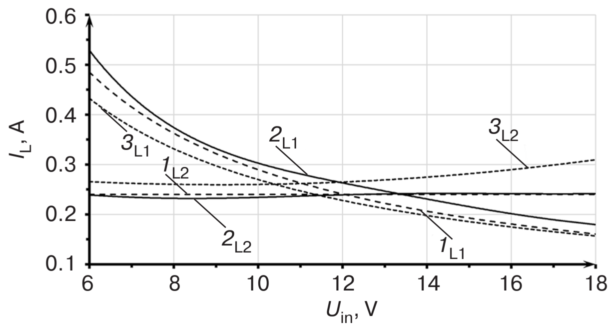

Fig. 9. Dependence of the constant currents flowing through the windings of chokes L1 and L2 on the input voltage U_{in} at a load resistance of 50 Ohm: *1* is calculation, *2* is modeling, and *3* is experimental

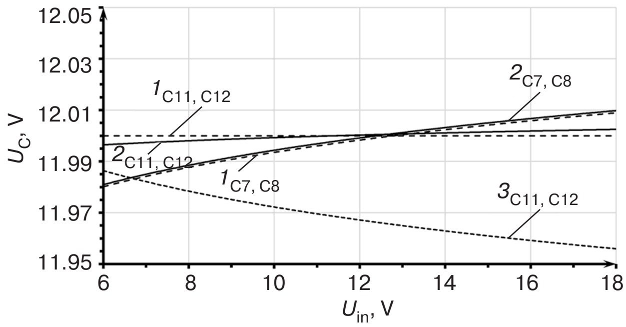

Fig. 10. Dependence of the voltages across the capacitors C7, C8 and C11, C12 on the input voltage U_{in} with a load resistance of 50 Ohm: *1* is calculation, 2 is modeling, and *3* is experimental

The graphs of the current ripple spreads Δi_{L1} and Δi_{L2} flowing through the windings of the inductors L1 and L2 as a function of the input voltage U_{in} (Fig. 11), as well as those of the voltage ripple spreads $\Delta u_{C7, C8}$ and $\Delta u_{C11, C12}$ (Fig. 12) across the capacitors C7, C8 and C11, C12 as a function of the input voltage U_{in} at a load resistance of 50 Ohm, show good agreement between the experimental and calculated values.

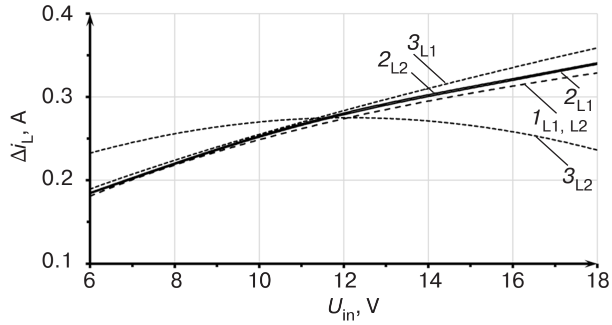

Fig. 11. Current ripple spreads through the windings of chokes L1 and L2 as a function of the input voltage U_{in} at a load resistance of 50 Ohm: *1* is calculated, *2* is modeling, and *3* is experimental

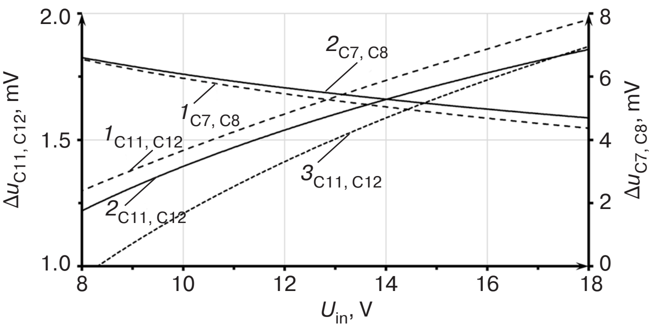

Fig. 12. Voltage ripple spreads across the capacitors C7, C8 and C11, C12 as a function of the input voltage U_{in} at a load resistance of 50 Ohm:
1 is calculation, *2* is modeling,
and *3* is experimental

Similar dependencies of the constant and alternating components of the currents i_{L1}, i_{L2} (Fig. 13) and the voltages $u_{C7, C8}$, $u_{C11, C12}$ (Fig. 14) on the input voltage U_{in} are obtained at a load resistance R_L = 100 Ohm. The deviation of the constant current components of I_{L1} is on average 16%, while the deviation of I_{L2} is 9.0% and the deviation of $u_{C11, C12}$ is 0.10%. For the ripple spreads of the corresponding currents and voltages, the following deviations are obtained: Δi_{L1} is 13%, Δi_{L2} is 30%, while $\Delta u_{C11, C12}$ is 38%.

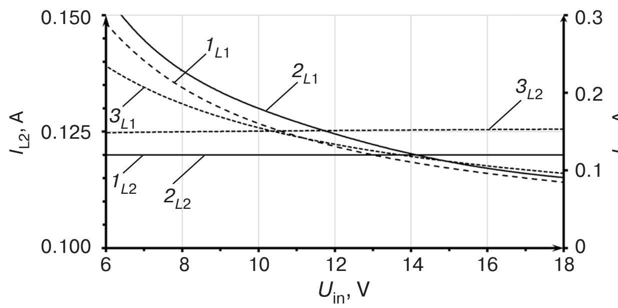

Fig. 13. Currents flowing through the windings of inductors L1 and L2 as a function of the input voltage U_{in} at a load resistance of 100 Ohm:
1 is calculation, *2* is modeling,
and *3* is experimental

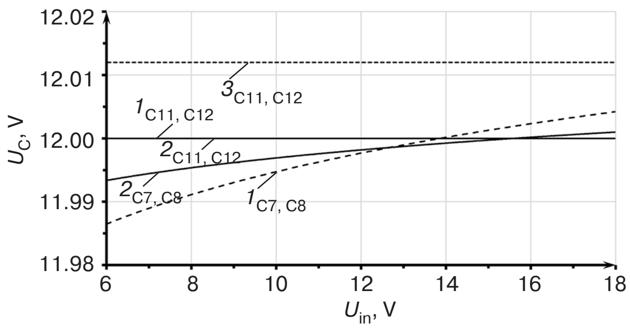

Fig. 14. Voltages across the capacitors C7, C8 and C11, C12 as a function of the input voltage U_{in} at a load resistance of 100 Ohm:
1 is calculation, *2* is modeling,
and *3* is experimental

The graphs of the current ripple spreads Δi_{L1} and Δi_{L2} flowing through the windings of the inductors L1 and L2 as a function of the input voltage U_{in} (Fig. 15) and of the voltage ripple spreads $\Delta u_{C7, C8}$ and $\Delta u_{C11, C12}$ (Fig. 16) across the capacitors C7, C8 and C11, C12 as a function of the input voltage U_{in} at a load resistance of 100 Ohm show good agreement between experimental and calculated values.

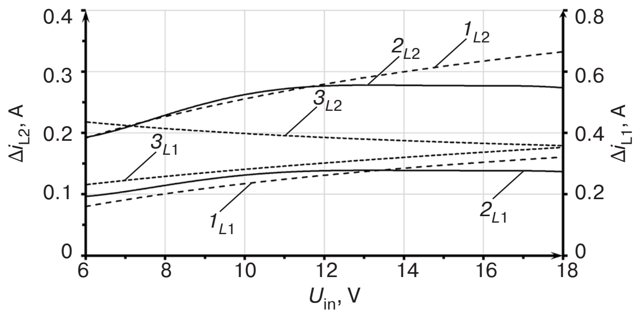

Fig. 15. Ripple currents flowing through the windings of chokes L1 and L2 as a function of the input voltage U_{in} at a load resistance of 100 Ohm:
1 is calculation, *2* is modeling, and *3* is experimental

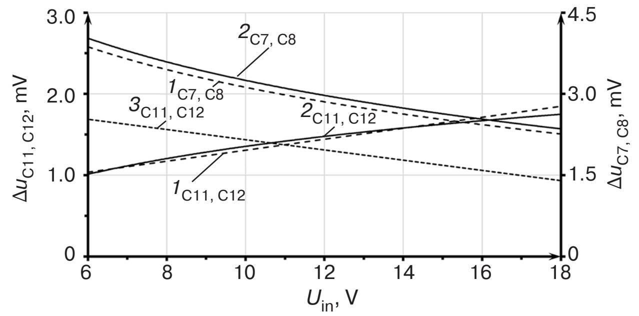

Fig. 16. Voltage ripple spreads across capacitors C7, C8 and C11, C12 as a function of the input voltage U_{in} at a load resistance of 100 Ohm:
1 is calculation, *2* is modeling, and *3* is experimental

The results of the study of the Zeta converter with inductively coupled chokes demonstrate the high correlation of both its LCs, as well as the dependence of the constant and alternating components of the currents i_{L1}, i_{L2} flowing through the windings of the chokes L1 and L2, and of the voltages $u_{C7, C8}$ and $u_{C11, C12}$ across the capacitors C7, C8 and C11, C12 on the input voltage U_{in} for two load resistances of 50 and 100 Ohm, which were obtained by different methods: experimental, calculated, and modeling. There is almost complete agreement between the calculated values and those obtained by SPICE[7] modeling. The differences between the experimental characteristics and those obtained by calculation and modeling can be considered negligible.

[7] SPICE (Simulation Program with Integrated Circuit Emphasis) is an open source simulator of general-purpose electronic circuits

CONCLUSIONS

We have described the design and construction a test bench of a DC/DC converter based on the Zeta topology with coupled chokes on the basis of a TPS40200 driver. An experimental study of the typical dependencies of the converter at different values of input voltage and load resistances was carried out. The experimental dependencies are compared with similar characteristics obtained by modeling using *Multisim* CAD and a calculation method based on the continuous-time mathematical model of the converter. A comparison of data obtained using these three methods demonstrates their high correlation.

Authors' contribution

All authors equally contributed to the research work

REFERENCES

1. Korotkov S.M., Lukin A.V. Power sources for LED lighting. *Prakticheskaya silovaya elektronika = Practical Power Electronics*. 2012;2(46):3–9 (in Russ.). https://www.elibrary.ru/papuhr
2. Obraztsov A., Obraztsov S. Circuit design of DC/DC converters. *Sovremennaya elektronika = Modern Electronics.* 2005;3:36–43 (in Russ.).
3. Bodin O.N., Bezborodova O.E., Mitroshin A.N., Chuvykin B.V., Martynov D.V., Edemskii M.V. Intelligent telemedicine information system. *Biomeditsinskaya radioelektronika = Biomedical Radioelectronics*. 2024;27(2):103–110 (in Russ.). https://doi.org/10.18127/j15604136-202402-14
4. Bityukov V.K., Simachkov D.S., Babenko V.P. *Skhemotekhnika elektropreobrazovatel'nykh ustroistv* (*Circuitry of Electrical Converter Devices*). Vologda: Infra-Inzheneriya; 2023. 384 p. (in Russ.). ISBN 978-5-9729-1439-5. https://www.elibrary.ru/pqyagy
5. Manannikova N.G., Shevtsov D.A. New Topology for the two-transistor power stage for a single-ended power converter. *Prakticheskaya silovaya elektronika = Practical Power Electronics*. 2023;1(89):17–20 (in Russ.). https://www.elibrary.ru/cuolqz
6. Anisimova T.V., Danilina A.N., Kryuchkov V.V. DC Boost Converter with Flying Capacitor. *Prakticheskaya silovaya elektronika = Practical Power Electronics*. 2021;1(81):28–33 (in Russ.). https://www.elibrary.ru/ijaakd
7. Minibaev L.M. Using zero ripple techniques in power supply designing. In: *Problems and Trends of Scientific Transformations in the Conditions of Society Transformation: Proceedings of the All-Russian Scientific and Practical Conference.* Ufa: Aeterna; 2020. P. 23–26 (in Russ.). https://www.elibrary.ru/pazzxq
8. Zhu F., Li Q. Coupled Inductors with an Adaptive Coupling Coefficient for Multiphase Voltage Regulators. *IEEE Trans. Power Electron*. 2023;38(1):739–749. https://doi.org/10.1109/TPEL.2022.3203855, https://www.elibrary.ru/hizbts
9. Zhang Ch., Yuan X., Wang J., et al. Si/WBG Hybrid Half-Bridge Converter Using Coupled Inductors for Power Quality Improvement and Control Simplification. *IEEE Trans. Power Electron*. 2024;39(3):3339–3352. https://doi.org/10.1109/TPEL.2023.3342133, https://www.elibrary.ru/kbwvtg
10. Tseng K.Ch., Huang G.Yu., Hsiung H.Yu. An isolated high step-down DC–DC converter with dual coupled inductors for ultracapacitor charger applications. *Int. J. Circuit Theor. Appl.* 2024;52(7):3341–3356. https://doi.org/10.1002/cta.3905, https://www.elibrary.ru/bfcarn
11. Bityukov V.K., Lavrenov A.I., Petrov D.R. Mathematical model of a ZETA-converter with inductively coupled chokes (Part 2). *Voprosy elektromekhaniki. Trudy VNIIEM = Elektromechanical Matters. VNIIEM Studies.* 2023;195(4):48–52 (in Russ.). https://elibrary.ru/mnusik
12. Bityukov V.K., Lavrenov A.I., Petrov D.R. Current and voltage pulsations of Zeta converter with inductively coupled inductors (Part 2). *Proektirovanie i tekhnologiya elektronnykh sredstv = Design and Technology of Electronic Means*. 2023;4:27–31 (in Russ.). https://www.elibrary.ru/dspqrt
13. Korshunov A.I. Limiting continuous model of a system with periodic high-frequency structure variation. *Silovaya elektronika = Power Electronics*. 2021;5(92):48−51 (in Russ.). https://www.elibrary.ru/sxwxqb
14. Belov G.A. Structural dynamic models of pulsed DC-DC switched mode converters in discontinuous current mode. *Prakticheskaya silovaya elektronika = Practical Power Electronics.* 2019;1(73):2–8 (in Russ.). https://www.elibrary.ru/jvniqr
15. Amelina M.A., Amelin S.A. Continuous Models of Composite DC-DC Converters. In: *Power Engineering, Computer Sciences, and Innovations – 2021: Proceedings of the 11th International Scientific and Technical Conference, Smolensk.* Smolensk: Universum; 2021. V. 1. P. 323–325 (in Russ.). https://www.elibrary.ru/klxdcg
16. Bityukov V.K., Lavrenov A.I. Method for designing DC/DC converters based on Zeta topology. *Russian Technological Journal.* 2025;13(1):59–67 (in Russ.). https://doi.org/10.32362/2500316X-2025-13-1-59-67

СПИСОК ЛИТЕРАТУРЫ

1. Коротков С.М., Лукин А.В. Источники питания для светодиодного освещения. *Практическая силовая электроника*. 2012;2(46):3–9. https://www.elibrary.ru/papuhr
2. Образцов А., Образцов С. Схемотехника DC/DC-преобразователей. *Современная электроника*. 2005;3:36–43.
3. Бодин О.Н., Безбородова О.Е., Митрошин А.Н., Чувыкин Б.В., Мартынов Д.В., Едемский М.В. Интеллектуальная телемедицинская информационная система. *Биомедицинская радиоэлектроника*. 2024;27(2):103–110. https://doi.org/10.18127/j15604136-202402-14
4. Битюков В.К., Симачков Д.С., Бабенко В.П. *Схемотехника электропреобразовательных устройств*. Вологда: Инфра-Инженерия; 2023. 384 с. ISBN 978-5-9729-1439-5. https://www.elibrary.ru/pqyagy
5. Мананникова Н.Г., Шевцов Д.А. Новая структура двухтранзисторного силового каскада для однотактного прямо-обратноходового преобразователя электроэнергии. *Практическая силовая электроника.* 2023;1(89):17–20. https://www.elibrary.ru/cuolqz
6. Анисимова Т.В., Данилина А.Н., Крючков В.В. Повышающий преобразователь постоянного напряжения с плавающим конденсатором. *Практическая силовая электроника*. 2021;1(81):28–33. https://www.elibrary.ru/ijaakd
7. Минибаев Л.М. Использовании техники нулевых пульсаций при проектировании источников питания. В сб.: *Проблемы и тенденции научных преобразований в условиях трансформации общества: сборник статей Всероссийской научно-практической конференции*. Уфа: Аэтерна; 2020. С. 23–26. https://www.elibrary.ru/pazzxq
8. Zhu F., Li Q. Coupled Inductors with an Adaptive Coupling Coefficient for Multiphase Voltage Regulators. *IEEE Trans. Power Electron*. 2023;38(1):739–749. https://doi.org/10.1109/TPEL.2022.3203855, https://www.elibrary.ru/hizbts
9. Zhang Ch., Yuan X., Wang J., et al. Si/WBG Hybrid Half-Bridge Converter Using Coupled Inductors for Power Quality Improvement and Control Simplification. *IEEE Trans. Power Electron*. 2024;39(3):3339–3352. https://doi.org/10.1109/TPEL.2023.3342133, https://www.elibrary.ru/kbwvtg
10. Tseng K.Ch., Huang G.Yu., Hsiung H.Yu. An isolated high step-down DC–DC converter with dual coupled inductors for ultracapacitor charger applications. *Int. J. Circuit Theor. Appl.* 2024;52(7):3341–3356. https://doi.org/10.1002/cta.3905, https://www.elibrary.ru/bfcarn
11. Битюков В.К., Лавренов А.И., Петров Д.Р. Математическая модель Zeta-преобразователя с индуктивно связанными дросселями (часть 2). *Вопросы электромеханики. Труды ВНИИЭМ*. 2023;195(4):48–52. https://elibrary.ru/mnusik
12. Битюков В.К., Лавренов А.И., Петров Д.Р. Пульсации токов и напряжений Zeta преобразователя с индуктивно связанными дросселями (часть 2). *Проектирование и технология электронных средств*. 2023;4:27–31. https://www.elibrary.ru/dspqrt
13. Коршунов А.И. Предельная непрерывная модель системы с периодическим высокочастотным изменением структуры. *Силовая электроника*. 2021;5(92):48–51. https://www.elibrary.ru/sxwxqb
14. Белов Г.А. Структурные динамические модели импульсных преобразователей постоянного напряжения в РПТ. *Практическая силовая электроника*. 2019;1(73):2–8. https://www.elibrary.ru/jvniqr
15. Амелина М.А., Амелин С.А. Непрерывные модели составных преобразователей постоянного напряжения. В сб.: *Энергетика, информатика, инновации – 2021: Сборник трудов XI Международной научно-технической конференции*. Т. 1. Смоленск: Универсум; 2021. С. 323–325. https://www.elibrary.ru/klxdcg
16. Битюков В.К., Лавренов А.И. Метод проектирования DC/DC-преобразователей, построенных по Zeta-топологии. *Russian Technological Journal*. 2025;13(1):59–67. https://doi.org/10.32362/2500316X-2025-13-1-59-67

About the authors

Vladimir K. Bityukov, Dr. Sci. (Eng.), Professor, Department of Radio Wave Processes and Technology, Institute of Radio Electronics and Informatics, MIREA – Russian Technological University (78, Vernadskogo pr., Moscow, 119454 Russia). E-mail: bitukov@mirea.ru. ResearcherID Y-8325-2018, Scopus Author ID 6603797260, RSCI SPIN-code 3834-5360, https://orcid.org/0000-0001-6448-8509

Aleksey I. Lavrenov, Postgraduate Student, Assistant, Department of Radio Wave Processes and Technology, Institute of Radio Electronics and Informatics, MIREA – Russian Technological University (78, Vernadskogo pr., Moscow, 119454 Russia). E-mail: lavrenov@mirea.ru. RSCI SPIN-code 6048-5027, https://orcid.org/0000-0001-5722-541X

Daniil A. Malitskiy, Circuit Engineer, SPUTNIX (Office 358, 359, 42/1, Bol'shoi bul'var, Skolkovo Technopark, Moscow, 121205 Russia). E-mail: malickij@mirea.ru. RSCI SPIN-code 4912-3018, https://orcid.org/0000-0003-4558-9085

Об авторах

Битюков Владимир Ксенофонтович, д.т.н., профессор, кафедра радиоволновых процессов и технологий, Институт радиоэлектроники и информатики, ФГБОУ ВО «МИРЭА – Российский технологический университет» (119454, Россия, Москва, пр-т Вернадского, д. 78). E-mail: bitukov@mirea.ru. Scopus Author ID 6603797260, ResearcherID Y-8325-2018, SPIN-код РИНЦ 3834-5360, https://orcid.org/0000-0001-6448-8509

Лавренов Алексей Игоревич, аспирант, ассистент, кафедра радиоволновых процессов и технологий, Институт радиоэлектроники и информатики, ФГБОУ ВО «МИРЭА – Российский технологический университет» (119454, Россия, Москва, пр-т Вернадского, д. 78). E-mail: lavrenov@mirea.ru. SPIN-код РИНЦ 6048-5027, https://orcid.org/0000-0001-5722-541X

Малицкий Даниил Александрович, инженер-схемотехник, ООО «СПУТНИКС» (121205, Россия, Москва, Технопарк «Сколково», Большой бульвар, д. 42, стр. 1, оф. 358, 359). E-mail: malickij@mirea.ru. SPIN-код РИНЦ 4912-3018, https://orcid.org/0000-0003-4558-9085

Translated from Russian into English by K. Nazarov
Edited for English language and spelling by Thomas A. Beavitt